ESTIMATION OF CURRENT DISTRIBUTIONS UNDER ELECTRODES FOR EXTERNAL DEFIBRILLATION AND PACING

Vessela Tzvetanova Krasteva, MScEE, PhD

Centre of Biomedical Engineering - Bulgarian Academy of Sciences
e-mail: vessika@clbme.bas.bg

Abstract

Thransthoracic electrical therapy of the heart is administered via large electrodes placed on specific locations on the thorax surface. A poor electrode-skin contact and a non-uniform current distribution under the electrodes may result in tissue damage and skin burns. In some cases skin irritation caused by long-term wearing of electrodes may occur. To lessen these adverse effects, the electrodes are interfaced to the skin by low-resistive conductive gel or solidified gel layer. Also, certain specific electrode designs could be used.

The present study is aimed at evaluation of the current density distribution under electrodes of different structure, e.g. shape, size, interfacing layer thickness and specific conductivity. A three-dimensional finite-element model was developed to solve the problems. We found that some complex electrode configurations lead to unacceptable current density distribution changes, thus reducing their efficiency.

Introduction

For the last 50 years the application of short-duration strong electrical pulses in the heart region has become a widespread method for resuscitation of persons in cardiac arrest [1]. The most accessible approach for electrical cardiac therapy is defibrillation or pacing via external electrodes, placed on specific locations on the thorax surface. These electrodes overlay a large area (70-120 cm^2) [2] and provide high and quazi-uniform current density distribution in the heart, which is necessary for synchronous excitation of most myocardial cells, thus forcing them to return to normal rhythm. Incorrect electrode placement results in disturbed inter-electrode impedance. For example, extreme closeness of electrodes causes the defibrillation pulse to be conducted across the surface, thus rendering it ineffective. Many authors investigate optimal electrode positions and sizes via bi-dimensional (2D) [3,4] and three-dimensional (3D) [5-7] finite-element method (FEM) models, with the aim to obtain uniform current distribution in the heart. The uniformity is evaluated by the ratio of the maximum current (which could result in myocardial damage) and the threshold current needed for defibrillation. For example Panescu et al. [6] reported that about 25% of the myocardium volume could be subjected to current densities more than 4 times higher than the threshold density.

Many cardiac arrest victims in asistoly need application of repeated electrical pulses to maintain effective cardiac rhythm during long periods of time. This procedure is accompanied with discomfort and even pain, associated with strong excitation of sensory nerve endings and skeletal muscles, thus provoking contractions [8]. It is evident that poor electrode-skin contact and non-uniform current distribution

under the electrodes (high current density along the perimeter) [9] may result in tissue damage and skin burns or electroporation [10]. The damage may persist several months. To reduce these adverse effects, the electrodes are covered with low-resistive gel or solidified gel layer [11]. Another problem is related to skin irritation, resulting from long-term application of the electrodes, when protective wearable defibrillator-monitor is used. In such cases certain specific electrode designs were developed, providing openings for improvement of skin aeration or "breathing" [12].

The aim of the present work is to evaluate the current density distribution profile under electrodes of different structure, including shape, size, interfacing layer thickness and specific conductivity.

Method

The steady state electrical potential V in an electrically conductive domain consisting of layers of different specific resistivities ρ, is governed by the pseudo-Laplace equation: $\frac{\partial}{\partial x}(\frac{1}{\rho}\frac{\partial V}{\partial x})+\frac{\partial}{\partial y}(\frac{1}{\rho}\frac{\partial V}{\partial y})+\frac{\partial}{\partial z}(\frac{1}{\rho}\frac{\partial V}{\partial z})=0$ (1). This equation is solved subject to the following boundary conditions:

- Dirichlet boundary conditions imposed on the surface SE_i in contact with the i_{th} electrode at potential V_i: $V(x,y,z)\,|\,SE_i = V_i$.
- Neumann boundary conditions state that the normal component of the derivative of the potential is zero in the remaining boundary plane (SB), not in contact with the electrodes: $(\frac{\partial V(x,y,z)}{\partial n})_{SB}=0$.

The current density distribution is defined by the potential gradient and the specific conductivity of the different regions: (2) $J(x,y,z)=\rho(-gradV(x,y,z))$.

In this study, a simplified 3D finite element model with over 50,000 eight-node tetrahedron elements (fig.1a) was developed to solve eqn (2). The measurements were taken 0.5 mm under the electrode-skin interface. The geometry of the thorax was simplified, simulated by a cylindrical domain (10 cm radius; 10 cm height) with specific resistivity of 20 Ω.m and estimated inter-electrode resistance of about 65 Ω, approximately corresponding to the real conditions in defibrillation. The electrodes, of ~80 cm^2 area and 1 mm thickness, were located on the upper and lower cylindrical surface. The defibrillation voltage was applied on the group of nodes forming the exterior electrode surface. The inter-electrode potential difference used in all comparative studies was set at 1000 V. The interfacing gel was simulated by thick (0.5-1.5 mm) low-resistivity (20 –60 Ω.m) layer under the electrodes (fig1b).

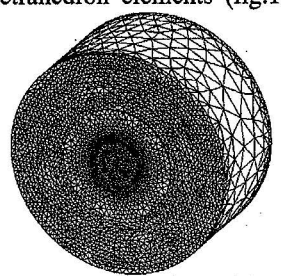

Fig.1a. 3D finite-element model

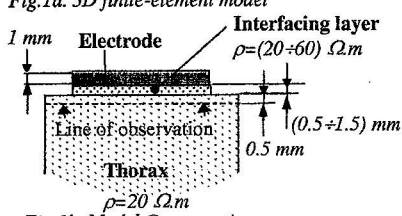

Fig.1b. Model Cross section

Results

1. Standard electrode configurations

The current distribution under the two most commonly used electrode types – square-shaped and circular, measured at 0.5 mm inside the thorax, is presented in fig.2. The interfacing layer, which follows the electrode shape, is chosen of 20 Ω.m specific resistivity and thickness of 0.5 mm. Thus the electrode-interface resistance of both electrodes does not exceed 2.5 Ω. The compared square-shaped (4.43 cm side) and circular (5 cm radius) electrodes are of equal of 80 cm^2 areas.

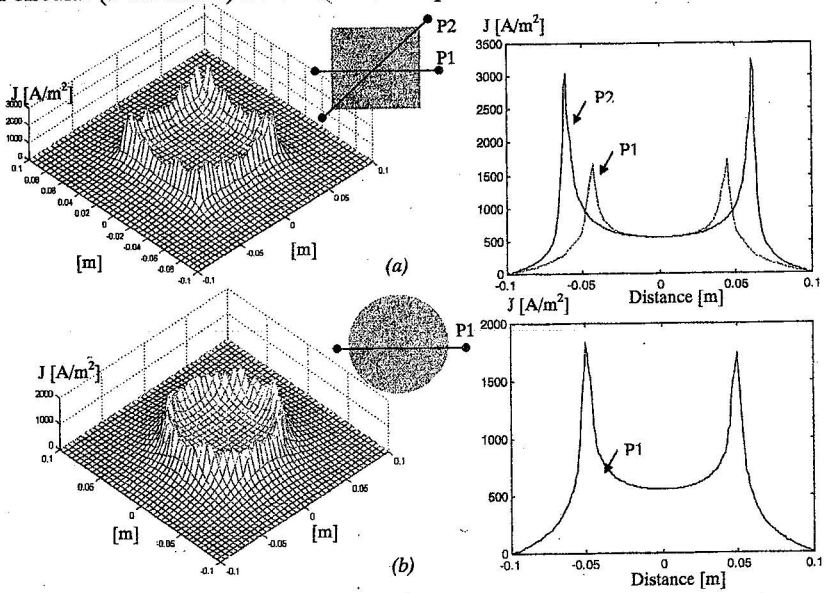

Fig.2. Current density distributions under square (a) and circular (b) electrodes of 80 cm^2 area
The right chart is a detailed profile along the path Pi

2. Circular electrode analysis

First the effect of the size of a circular electrode was examined. Two electrodes were designed - of 5 cm radius and a twice-shorter 2.5 cm radius. The respective current distributions are shown in fig.3a. Takings into account the "non-uniformity coefficient", i.e. the ratio (K) between the maximum current J_{max} to the minimum current J_{min}, the results of the comparison are represented in Table 1.

Electrode Radius [cm]	Interfacing layer (5mm thickness)		J_{max}/J_{min} [A/m^2]	$K=J_{max}/J_{min}$
	ρ [Ω.m]	R [Ω]		
5	20	1.25	1780/570	3.12
5	80	5.1	1490/550	2.71
2.5	20	5.1	2150/780	2.76
2.5	4	1.25	2450/800	3.06

Table1

In an attempt to obtain a more uniform current distribution, an additional (2mm) interfacing ring-shaped layer with higher specific resistivity (ρ=100 Ω.m) was added around the electrode periphery . It can be seen (fig.3b) that thus the maximum current density along the electrode perimeter was reduced by 12 % and the non-uniformity coefficient dropped to K=2.77 (1580/570 A/m^2), achieved without increasing the resistance in the current pathway.

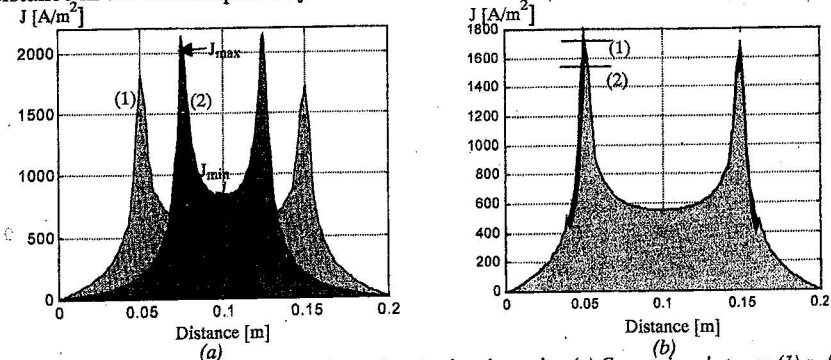

Fig.3.Current density distribution profiles under circular electrodes. (a) Comparison between (1) r=5 cm and (2) r=2.5 cm, with interfacing layer ρ=20 Ω.m, thickness of 0.5 mm. (b) Comparison between (1) r=5 cm and (2) r=5cm and an additional surrounding ring of ρ=100 Ω.m.

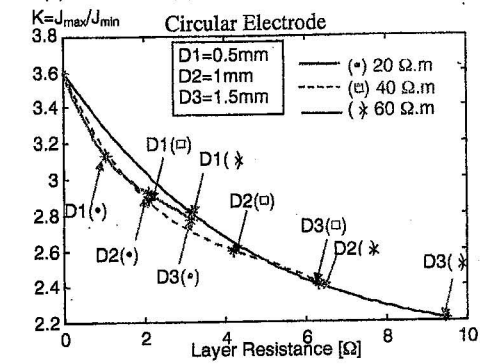

Fig.4.
D(1,2,3) – interfacing layer thickness; (•,□,x) - resistivity

The next step was to examine the influence of the interfacing layer thickness and specific resistivity ρ. A 5 cm radius electrode was chosen for this analysis. Nine measurements were taken: three for ρ=20 Ω.m (interface thickness 0.5, 1 and 1.5 mm), and three more, each for ρ=40 and ρ=60 Ω.m. The results for the estimated "non-uniformity" coefficient K as a function of the overall electrode-interface resistance, are presented in fig.4.

3. *Other electrode types*

The performance of electrodes of different shapes is shown in fig.5. The electrodes of fig.5 a-c are similar to the circular electrode (radius 5cm; interfacing layer thickness=0.5 mm, ρ=20 Ω.m), but are provided with openings for improvement of the skin aeration. We decided to experiment an electrode where the openings (fig. 5a) were replaced with conductive elements, with results shown in fig. 5d. The four circular electrodes in fig.5e, each of them surrounded by an additional

ring (as for the single-disk electrode -fig. 3b), are of the same area as the basic circular electrode.

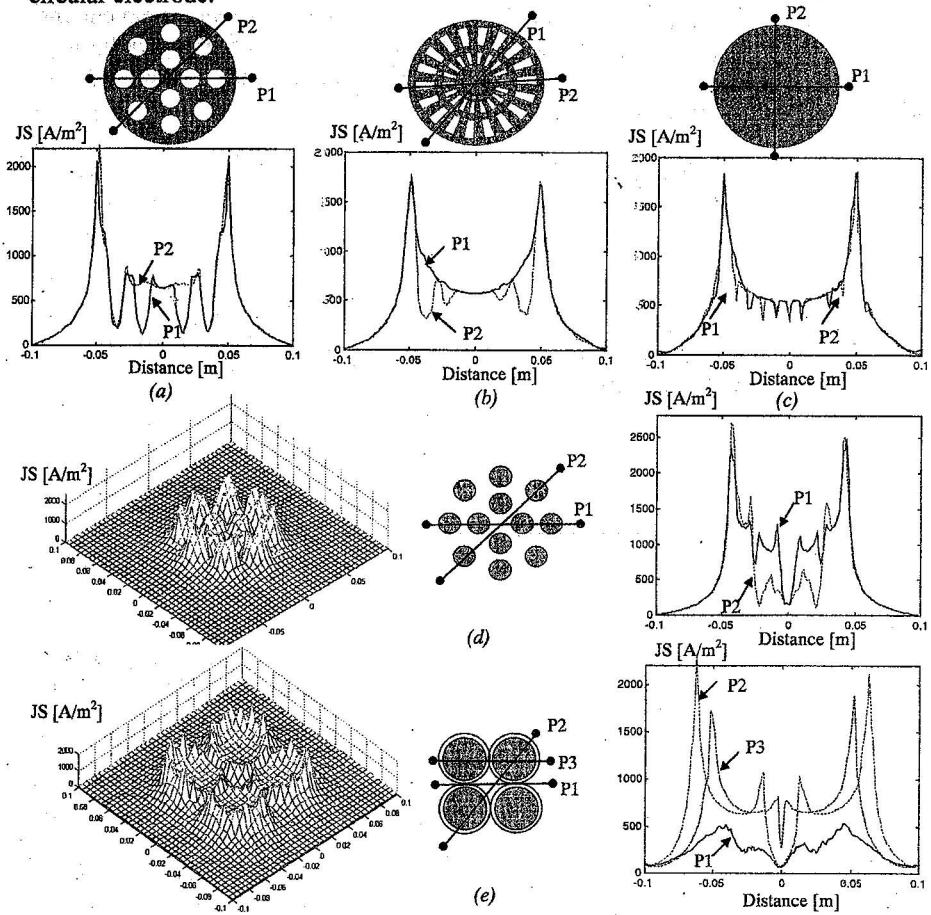

Fig.5.Current density distribution profiles under different electrode configurations. The paths of observation Pi are shown on the respective electrode shape view. (d) and (e) include also the current distributions in a cut-off area, located 0.5 mm under the interfacing layer inside the thorax.

Discussion and conclusion

The commonly used rectangular electrodes (area ~80 cm^2) show a high non-uniformity of the current distribution. Its profile across the corners shows a 4.6 times higher current density, compared to the density in the central region (fig.2a). The standard circular electrode with the same area yields 32% less non-uniformity (fig.2b). The influence of the electrode size is related to higher current density values under smaller electrodes (fig.3a). However, the electrode radius cannot be under 4.5

cm for the minimum area of 70 cm^2, recommended for ensuring a sufficient current density to depolarize a critical mass of myocardium.

The resistance of the electrode-skin interfacing layer is the major determinant of the maximum current in the distribution profile. Two electrodes with different sizes show equal non-uniformity, assessed by the coefficient $K = J_{max}/J_{min}$, if the under-electrode layer specific resistivity is chosen to provide the same electrode resistance (table1). This result was confirmed also for interfacing layers of different thickness. For example, a thick layer with lower specific resistance has the same behavior as a thin layer with higher ρ (fig.4). This result didn't confirm our expectations that the thickness of the interface has a major straightening effect on the current lines. The higher resistance is associated with less non-uniformity, but the electrode configuration must not add more than 3-5% to the total resistance of the defibrillation current path. Many authors investigated the advantage of covering the electrode metal with resistive layers of increasing resistivity toward the periphery [9,13,14]. Such a technique seems technologically difficult and expensive for production of electrodes. We propose a simpler approach, by adding a ring of higher resistivity along the electrode perimeter. Thus the total resistance in the current pathway is not increased and the maximum periphery current is reduced with 12%. The same result could be achieved with 3 times higher resistance of an uniform layer.

Various electrode shapes, which provide openings for skin "breathing" (fig.5), increase the effect of non-uniformity, as the current density under the gaps drops strongly. The electrode of fig5c provides a more acceptable distribution.

References:

1. International Liaison Committee on Resuscitation, 2000, Guidelines 2000 for Cardiopulmonary Resuscitation and Emergency Cardiovascular Care, Circulation, 102:I-90. .
2. Windle J.R., Easley A.R., Stratbucker R.S., 1992, A multipurpose, self adhesive patch electrode capable of external pacing cardioversion defibrillation and 12-lead EKG, In: Birkui, Trigano, Zoll (eds.): Noninvasive transcutaneous cardiac pacing, Mount Kisco, New York, Futura Publishing Company, Inc., 179-191.
3. Fahy B.J. et al., 1987, Optimal electrode configurations for external cardiac pacing and defibrillation: an inhomogeneous study, IEEE Transactions on Bio-Med. Eng., 34,743-748.
4. Lehr J.L. et al, 1992, Test of four defibrillation dosing strategies using a two-dimensional finite-element model, Med&Biol. Eng,&Comp., 30, 621-628.
5. Camacho M.A. et al., 1995, A three-dimensional finite element model of human transthoracic defibrillation: paddle placement and size, IEEE Transactions on Bio-Med. Eng., 42, 572-578.
6. Panescu D. et al., 1995, Optimization of cardiac defibrillation by three dimensional finite element modelling of the human thorax, IEEE Transactions on Bio-Med. Eng.,42, 185-191.
7. Jorgenson D.B. et al, 1995, Computational studies of transthoracic and transvenous defibrillation in a detailed 3D human thorax model, IEEE Transactions on Bio-Med. Eng., 42, 172-183.
8. Falk R. H., Zoll P. M. and Zoll R. H., 1983, Safety and efficacy of noninvasive cardiac pacing. A preliminary report. New England Journal of Medicine, 309, 1166-1168.
9. Wiley J.D., Webster J.G., 1982, Analysis and control of the current distribution under circular dispersive electrodes, IEEE Transactions on Bio-Med. Eng., 29, 381-385.
10. Vogel U. et al., 1998, Extensive pectoral muscle necrosis after defibrillation: nonthermal skeletal muscle damage caused by electroporation, Intensive Care Medicine , 24, 743-745.
11. Amato-Vealey E., Colonies P.A., 2001, Demystifying biphasic defibrillation, Nursing management, 4-15.
12. Owen J.M. et al. 2002, Defibrillation system, Patent N US 6,374,138 B1.
13. Kim Y., 1996, Electrical behavior of defibrillation and pacing electrodes, Proceedings of the IEEE, 84, 446-456.
14. Papzov S. et al., Electrical current distribution under transthoracic defibrillation and pacing electrodes, J.Med. Eng.&Technol., 26, 22-27.